https://doi.org/10.3311/PPee.20384
Creative Commons Attribution

Periodica Polytechnica Electrical Engineering and Computer Science, 67(1), pp. 1–9, 2023

A Highly Effective Modified Direct Torque Control for Five Phase Induction Motor without AC Phase Current Sensors

Ahmed Azib[1*], Djamel Ziane[1,2]

[1] Laboratoire de Technologie Industrielle et de l'information (LTII), Faculté de Technologie, Université de Bejaia, 06000 Bejaia, Algeria
[2] Département d'Electrotechnique, Faculté de Génie Électrique et d'Informatique, Université Mouloud Mammeri de Tizi-Ouzou, 15000 Tizi-Ouzou, Algeria
* Corresponding author, e-mail: ahmed.azib@univ-bejaia.dz

Received: 27 April 2022, Accepted: 22 September 2022, Published online: 13 October 2022

Abstract

The Direct Torque Control (DTC) technique requires stator currents and DC bus voltage, as well as inverter switch states, in order to estimate stator flux and electromagnetic torque values. Measurement of phase currents in real time with current sensors is a common method of gathering this data. To control a Five-Phase Induction Motor (FPIM), the DTC needs at least four alternating current (AC) sensors and one voltage sensor. When utilized in a global training system, this number has disadvantages due to cost, size, and non-linearity. The purpose of this article is to show how to remove the alternating current sensors from an FPIM's DTC. This is accomplished by reconstructing the phase currents using a simple DC current sensor placed at the voltage inverter's input and modifying the classical DTC control technique by using a good choice of certain allowable switching vectors of a five-phase voltage inverter, the 18° zone offset strategy of the stator flux, and developing a new commutation table for the stator currents construction. The proposed control approach is supported by simulation results.

Keywords

direct torque control, five-phase induction motor, alternating current sensor, direct current sensor, five phase voltage inverter

1 Introduction

The technological development of static power converters capable of delivering adjustable frequencies allows the three-phase AC motor to be used as the main driving machine for a very long time. However, this converter-machine assembly is still restricted to the lower limit of the high power range due to the electrical stresses on the semiconductors and their low switching frequency.

However, in order to provide electric drive for applications requiring a higher power level, beyond several tens of megawatts, the solution consists of the use of electric machines with more than three phases, i.e., polyphase machines, since they offer many potential advantages compared to their three-phase counterparts [1, 2]. These benefits are mainly related to: increased fault tolerance; higher powers achieved through power segmentation; improved drive performance in terms of efficiency and torque ripples [3].

The first vector control method of an AC motor was the flux oriented method presented by "Hasse (IFOC) [4]" and "Blaschke (FOC) [5] in the early 70s". These methods have been studied and discussed by many researchers and have now become standard for the industry. The FOC method guarantees the decoupling of flux and torque. However, its main disadvantages are: the large computing capacity required and the mandatory identification of the machine parameters.

In the mid-1980s new control strategies for induction motor torque control were introduced by "Takahashi and Noguchi as Direct Torque Control (DTC) [6]" and by "Depenbrock as Direct Self Control (DSC) [7, 8]". These methods, thanks to the alternative approach to induction motor control, have become alternatives for classical vector control - FOC.

Indeed, excellent dynamic performance and structural simplicity are the main features of conventional direct torque control. However, the classic DTC has several disadvantages, the most important of which is the variable switching frequency operation and using current sensors. Generally, current sensors with galvanic isolation such as Hall Effect sensors and current transducers are widely used in many applications. Such a type of sensor works

Cite this article as: Azib, A., Ziane, D. "A Highly Effective Modified Direct Torque Control for Five Phase Induction Motor without AC Phase Current Sensors", Periodica Polytechnica Electrical Engineering and Computer Science, 67(1), pp. 1–9, 2023. https://doi.org/10.3311/PPee.20384

well, but brings disadvantages to the overall training system in terms of cost, size and non-linearity [9, 10].

In recent years, another scheme of AC sensorless DTC control has been proposed for three-phase AC machines [11]. In this new method, a suitable method to reconstruct phase currents and voltages from a single current sensor placed at the input of the inverter is designed, with a double modification of the classical DTC technique by using in the first a simple strategy of moving the sectors of the stator flux and in the second modification, the control system should be able to generate additional voltage vectors. This objective can be achieved by applying to each period different voltage vectors in predetermined time intervals, leading to the technique of discrete vector modulation.

We are interested in this article in the study and application of DTC control without alternating current sensors to the driving of the FPIM by a modification of the classic DTC control. The simulation study is carried out under the Simulink environment of MATLAB.

2 General principles of Direct Torque Control

The DTC of a polyphase machine is based on the direct determination of the command sequence applied to the switches of a voltage inverter. This choice is generally based on the use of hysteresis regulators whose function is to control the state of the system, namely here the amplitude of the flux of the stator and the electromagnetic torque [12, 13].

3 Direct torque control of five phase induction motor

The block diagram of the DTC control of a FPIM is shown in Fig. 1; the FPIM is connected to a five-phase inverter. This inverter is made up of five branches, each made up of two pairs of switches, assumed to be perfect and whose controls are complementary; each switch is modeled by two states defined by the following logic function:

$$s_i = \begin{cases} 1 \text{ if } s_i \text{ is closed} \\ 0 \text{ if } s_i \text{ is open} \\ \text{with } i = a,b,c,d \text{ and } e \end{cases}.$$

Then the phase-to-neutral output voltages as a function of the states of the switches give the following matrix system:

$$\begin{bmatrix} V_a \\ V_b \\ V_c \\ V_d \\ V_e \end{bmatrix} = \sqrt{\frac{2}{5}}U \begin{bmatrix} 4 & -1 & -1 & -1 & -1 \\ -1 & 4 & -1 & -1 & -1 \\ -1 & -1 & 4 & -1 & -1 \\ -1 & -1 & -1 & 4 & -1 \\ -1 & -1 & -1 & -1 & 4 \end{bmatrix} \cdot \begin{bmatrix} S_a \\ S_b \\ S_c \\ S_d \\ S_e \end{bmatrix}. \quad (1)$$

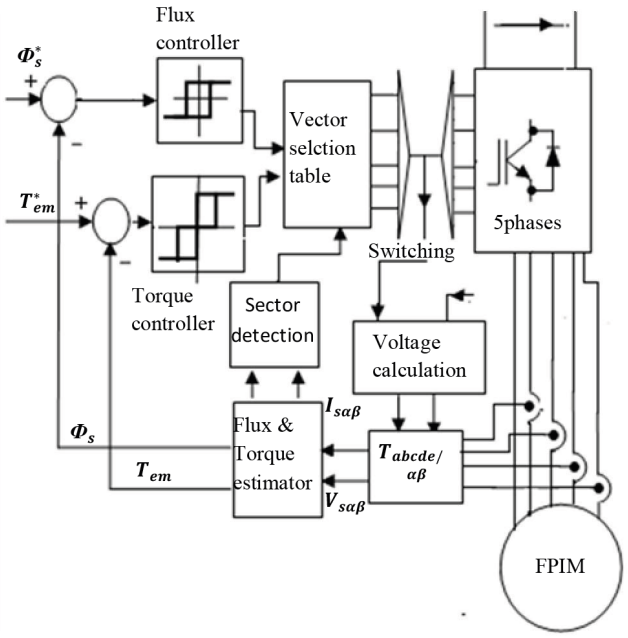

Fig. 1 Schematic diagram of the DTC of a FPIM

3.1 Operation and sequences of a five-phase voltage inverter

A five phase voltage inverter achieves thirty-one distinct positions in the phase plane, corresponding to the thirty-two sequences of the output voltage of the inverter, we can write [14, 15]:

$$V_i = \begin{cases} \sqrt{\frac{2}{5}} V_{pn} e^{j(s-1)\pi/5} & i = 25,17,19,3,7,6,14,12,28,24 \\ \frac{2}{5} V_{pn} e^{j(s-1)\pi/5} & i = 16,27,1,23,2,15,4,30,8,29 \\ \left(\sqrt{\frac{2}{5}} - \frac{2}{5}\right) V_{pn} e^{j(s-1)\pi/5} & i = 9,21,18,11,5,22,10,13,20,26 \\ 0 & i = 0,31 \text{ and } s = 1\ldots10 \end{cases}. \quad (2)$$

The 32 sequences are divided into 30 active vectors (V_1 to V_{30}) and two zero vectors (V_0 and V_{31}), and are represented in the complex plane (α-β) as shown in Fig. 2.

We will therefore seek to control the flux and the torque via the choice of the voltage vector which will be done by a configuration of the switches. By imposing that the active vectors which have a median amplitude (V_{16}, V_{27}, V_1, V_{23}, V_2, V_{15}, V_4, V_{30}, V_8, and V_{29}) and two vectors (V_0 and V_{31}) correspond to zero vectors. The representation of these vectors on the plane α-β is given by Fig. 3.

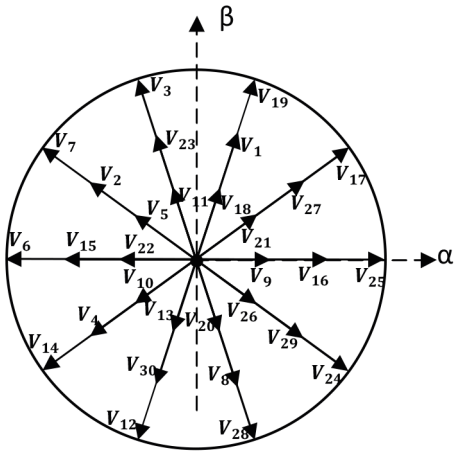

Fig. 2 Representation of the switching vectors of the five-phase inverter

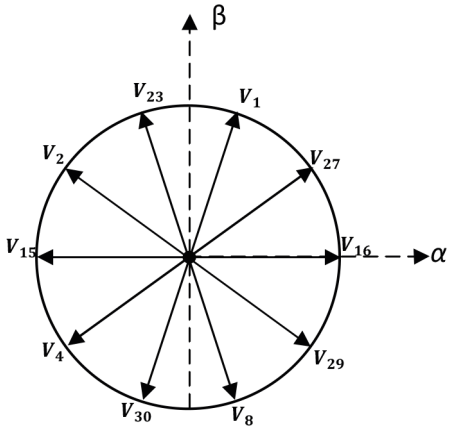

Fig. 3 Active vectors which have median amplitude for the five-phase inverter

3.2 Voltage vector selection

In order to fix the magnitude of the stator flux vector, the end of the flux vector must have a circular trajectory. For this, the voltage vector applied must always be perpendicular to the flux vector. But as we only use ten vectors, we have to accept an amplitude variation around the desired value.

The choice of vector $\boldsymbol{V}_s$ depends on the position of the vector $\boldsymbol{\Phi}_s$, of the desired variation for the modulus of the vector $\boldsymbol{\Phi}_s$, the variation desired for the torque, and the direction of rotation of $\boldsymbol{\Phi}_s$.

The complex plane α-β fixed to the stator is subdivided into ten sectors S_i, with $i = 1\ldots10$ such as:

$$(2i-3)\frac{\pi}{10} \le S_i \le (2i-1)\frac{\pi}{10}.$$

Each sector S_i will contain an active space vector $\boldsymbol{V}_i$ of inverter voltage as shown in the diagram in Fig. 4. The flux then rotates counterclockwise.

When the flux vector is in the area numbered i and the motor is rotating counterclockwise, the voltage vector $\boldsymbol{V}_{i+1}$ is chosen to increase both the stator flux and the electromagnetic torque. The vector $\boldsymbol{V}_{i+2}$ is chosen to increase the torque but reduce the stator flux. The two zero voltage vectors ($\boldsymbol{V}_0$ and $\boldsymbol{V}_{31}$) are used to reduce the torque and at the same time block the stator flux. Vector $\boldsymbol{V}_{i-2}$ is used to decrease torque and flux in brake mode and vector $\boldsymbol{V}_{i-1}$ reduces torque and increases flux. Fig. 4 shows an example of the stator flux vector located in sector 1 with the voltage vectors.

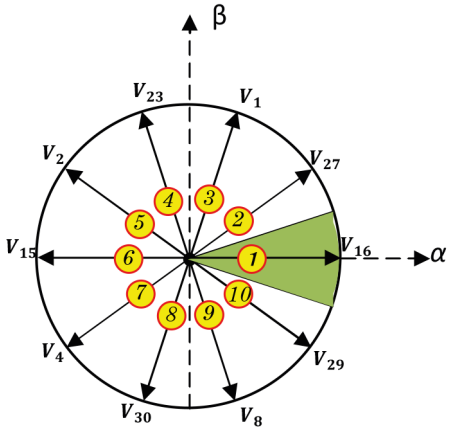

Fig. 4 Selection of the voltage vector according to zone i

3.3 Flux and torque estimation

3.3.1 Stator flux estimation

The flux estimate is made from measurements of the stator quantities (current and voltage) of the machine.

From Eq. (3):

$$\boldsymbol{\Phi}_s = \int_0^t (V_s - r_s i_s)\,\mathrm{d}t\,, \tag{3}$$

we obtain the components α and β of the vector $\boldsymbol{\Phi}_s$

$$\begin{cases} \Phi_{s\beta} = \int_0^t (V_{s\beta} - r_s I_{s\beta})\,\mathrm{d}t \\ \Phi_{s\beta} = \int_0^t (V_{s\beta} - r_s I_{s\beta})\,\mathrm{d}t \end{cases}. \tag{4}$$

The voltages $V_{s\alpha}$ and $V_{s\beta}$ are obtained from the commands s_a, s_b, s_c, s_d, s_e and from the measurement of the voltage V_{pn} with the application of course of the CLARKE transform:

$$V_s = V_{s\alpha} + jV_{s\beta} \tag{5}$$

$$\begin{cases} V_{s\alpha} = \frac{2}{5}V_{pn}\left(s_a + \cos\left(\frac{2\pi}{5}\right)(s_b + s_e) + \cos\left(\frac{4\pi}{5}\right)(s_c + s_d)\right) \\ V_{s\beta} = \frac{2}{5}V_{pn}\left(\sin\left(\frac{2\pi}{5}\right)(s_e - s_b) + \sin\left(\frac{4\pi}{5}\right)(s_d - s_c)\right) \end{cases}. \tag{6}$$

Similarly, the currents $I_{s\alpha}$ and $I_{s\beta}$ are obtained from the measurement of the real currents i_{sa}, i_{sb}, i_{sc}, i_{sd} and i_{se} such that $i_{sa} + i_{sb} + i_{sc} + i_{sd} + i_{se} = 0$ and by the application of the CLARKE transform:

$$i_s = I_{s\alpha} + jI_{s\beta} \tag{7}$$

$$\begin{cases} I_{s\alpha} = \frac{2}{5}\left(i_a + \cos\left(\frac{2\pi}{5}\right)(i_b + i_e) + \cos\left(\frac{4\pi}{5}\right)(i_c + i_d)\right) \\ I_{s\beta} = \frac{2}{5}\left(\sin\left(\frac{2\pi}{5}\right)(i_e - i_b) + \sin\left(\frac{4\pi}{5}\right)(i_d - i_c)\right) \end{cases}. \tag{8}$$

The modulus of the stator flux of a FPIM is written:

$$\mathbf{\Phi}_s = \sqrt{\left(\Phi_{s\alpha}\right)^2 + \left(\Phi_{s\beta}\right)^2}\ . \tag{9}$$

The zone (i) in which the vector $\mathbf{\Phi}_s$ is located is determined from the components $\Phi_{s\alpha}$ and $\Phi_{s\beta}$. The angle (θ_{sr}) is equal:

$$\theta_{sr} = \tan^{-1}\left(\frac{\Phi_{s\beta}}{\Phi_{s\alpha}}\right). \tag{10}$$

3.3.2 Electromagnetic torque estimation

The electromagnetic torque can be estimated only from the flux and current stator quantities. Thus, from the components (α, β) of the flux and current quantities, the torque can be put in the form:

$$T_{em} = \frac{5}{2} p\left(\Phi_{s\alpha} I_{s\beta} - \Phi_{s\beta} I_{s\alpha}\right). \tag{11}$$

3.4 Elaboration of the commutation table

According to the DTC principle, the correct selection of the voltage vector, at each sampling period, is made to maintain the torque and the flux within the limits of the two hysteresis bands. In particular, the selection is made based on the instantaneous flux error e_Φ, the torque error e_T and according to the stator flux vector position.

The optimal selection of switching vectors in all plane sectors of the stator flux can be represented in the form of a Table 1.

4 Direct torque control algorithm of FPIM without AC sensors

4.1 Measurement of phase currents for DTC control

To estimate the values of the stator flux and the electromagnetic torque, the DTC technique control requires information about stator currents and the DC bus voltage which is used with the switch states of the inverter. So the stator currents information is generally obtained by instantaneous measurement of phase currents using current sensors. Generally, current sensors with galvanic isolation such as Hall Effect sensors and current transducers are widely used in many applications. Such a type of sensor works well, but brings disadvantages to the overall training system in terms of cost, size and non-linearity [12, 13].

4.2 Technique of DTC control without alternating current sensors

The conventional direct torque control technique for FPIM requires at least four current sensors. The proposed scheme of the DTC control described in this article uses a simple DC current sensor to measure the DC bus current at the input of the inverter Fig. 5.

To this end, we choose from 32 voltage vectors of five phase inverter only 10 which enable us to measure one of the five phase currents, and then we elaborate a suitable method to reconstruct the phase currents by a simple modification of the classical DTC technique, using a simple strategy of displacements of the sectors of the stator flux.

Two modifications of the classic DTC control technique are used to estimate the five phase currents from a single current sensor placed at the input of the inverter. In the first modification, the control system should be able to generate additional voltage vectors. This objective can be achieved by applying to each period different voltage vectors in predetermined time intervals, leading to the technique of discrete vector modulation. By using this modulation strategy, new voltage vectors can be synthesized compared to those used in the classical DTC control technique.

It has been verified that the subdivision of the sampling period into four equal time intervals leads to a reduction in the number of current sensors without the need for more complex commutation tables. In addition, 40 new voltage

Table 1 Four-quadrant switching table for conventional DTC algorithm

e_Φ	e_T	①	②	③	④	⑤	⑥	⑦	⑧	⑨	⑩
1	1	V_{27}	V_1	V_{23}	V_2	V_{15}	V_{30}	V_8	V_{29}	V_{16}	V_4
	0	V_{29}	V_{16}	V_{27}	V_1	V_{23}	V_2	V_{15}	V_4	V_{30}	V_8
0	1	V_{23}	V_2	V_{15}	V_4	V_{30}	V_8	V_{29}	V_{16}	V_{27}	V_1
	0	V_4	V_{30}	V_8	V_{29}	V_{16}	V_{27}	V_1	V_{23}	V_2	V_{15}

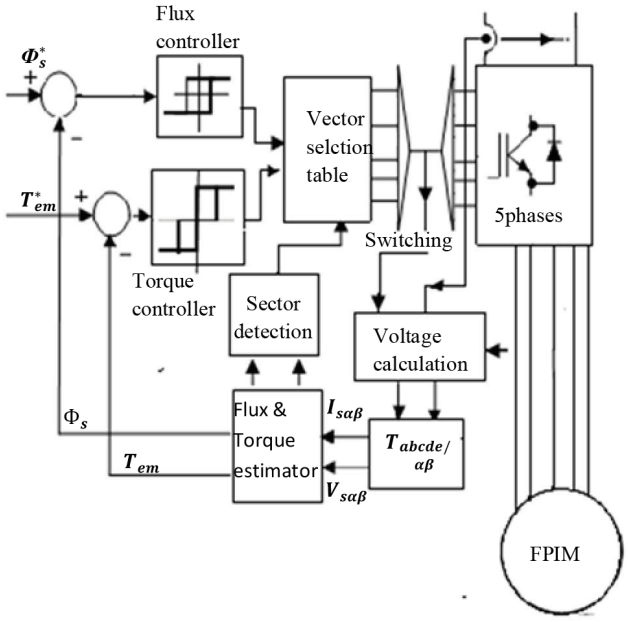

Fig. 5 Synoptic diagram of the proposed DTC control

vectors can be generated and only ten of them are used in the proposed DTC algorithm as shown in Fig. 6. The vectors in red color represent the synthesized voltage vectors.

The second modification allowing the improvement of the classic DTC control is the elaboration of the new commutation table by adjusting the ten sectors of the stator flux of the classic DTC control. The first sector is taken from 0° to 36° Fig. 7, instead of −18° to 18°. The new commutation table is presented in Table 2.

4.3 Elaboration of the commutation table

The new optimal selection of switching vectors in all plane sectors of the stator flux can be represented in the form of a Table 2.

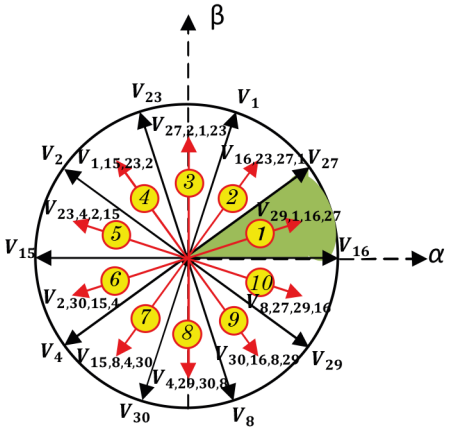

Fig. 6 Selection of the voltage vector according to the sectors of the proposed DTC control

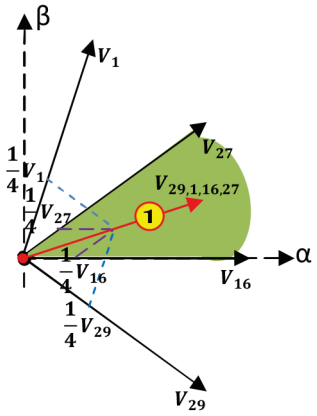

Fig. 7 The first sector is taken from 0° to 36°

4.4 Reconstruction of inverter output currents

In classic DTC, for each active voltage vector, there is only one current flowing in the intermediate circuit, which can be measured. Table 3 presents, according to the voltage vector applied the relationship between the DC bus intermediate circuit current and the phase currents.

By using discrete vector modulation at four intervals for each of the ten new active vectors, the five-phase currents of the motor can be reconstructed Table 4.

From Table 4, it is clear that by knowing the states of the inverter switches in the four intervals of each period, the actual currents for four phases can be obtained easily. Assuming that, I_{dc1} is the DC bus current measured at the end of the first interval, I_{dc2} is that measured during the second interval, I_{dc3} is that measured at the end of the third interval and I_{dc4} is that measured during the fourth interval.

The five motor phase currents I_a, I_b, I_c, I_d and I_e are given as a function of the voltage vector and the DC link current in Table 5. An example of a reconstruction sequence of phase currents at the application of the voltage vector $V_{29,1,16,27}$ is shown in Fig. 8.

5 Simulation results

The simulation of the proposed diagram of the DTC command described in this article is carried out under MATLAB/SIMULINK.

The value of the sampling interval of the DTC algorithm adopted in the simulation is $Te = 1e - 5$.

Fig. 9 illustrates the motor torque variations under the proposed control system. At the beginning, the torque reference is imposed at 20 N m, then a torque reversal occurs at 0.5 s, according to the pace we notice that the torque has a good dynamic.

Table 2 Switching table for proposed DTC algorithm

e_Φ	e_T	1	2	3	4	5	6	7	8	9	10
1	1	$V_{27,23,27,1}$	$V_{27,2,1,23}$	$V_{1,15,23,2}$	$V_{23,4,2,15}$	$V_{2,30,15,4}$	$V_{15,8,4,30}$	$V_{4,29,30,8}$	$V_{30,16,8,29}$	$V_{8,27,29,16}$	$V_{29,1,16,2}$
	0	$V_{8,27,29,16}$	$V_{29,1,16,27}$	$V_{16,23,27,1}$	$V_{27,2,1,23}$	$V_{1,15,23,2}$	$V_{23,4,2,15}$	$V_{2,30,15,4}$	$V_{15,8,4,30}$	$V_{4,29,30,8}$	$V_{30,16,8,2}$
0	1	$V_{1,15,23,2}$	$V_{23,4,2,15}$	$V_{2,30,15,4}$	$V_{15,8,4,30}$	$V_{4,29,30,8}$	$V_{30,16,8,29}$	$V_{8,27,29,16}$	$V_{29,1,16,27}$	$V_{16,23,27,1}$	$V_{27,2,1,23}$
	0	$V_{15,8,4,30}$	$V_{4,29,30,8}$	$V_{30,16,8,29}$	$V_{8,27,29,16}$	$V_{29,1,16,2}$	$V_{16,23,27,1}$	$V_{27,2,1,23}$	$V_{1,15,23,2}$	$V_{23,4,2,15}$	$V_{2,30,15,4}$

Table 3 The currents measured for each voltage vector of the classic DTC

Active Voltage Vector	DC-Link current
V_{16}	I_a
V_{27}	$-I_c$
V_1	I_e
V_{23}	$-I_b$
V_2	I_d
V_{15}	$-I_a$
V_4	I_c
V_{30}	$-I_e$
V_8	I_b
V_{29}	$-I_d$

Table 4 The currents measured for each voltage vector of the proposed DTC

Active Voltage Vector	1st DC-Link current	2nd DC-Link current	3rd DC-Link current	4th DC-Link current
$V_{29,1,16,27}$	$-I_d$	I_e	I_a	$-I_c$
$V_{16,23,27,1}$	I_a	$-I_b$	$-I_c$	I_e
$V_{27,2,1,23}$	$-I_c$	I_d	I_e	$-I_b$
$V_{1,15,23,2}$	I_e	$-I_a$	$-I_b$	I_d
$V_{23,4,2,15}$	$-I_b$	I_c	I_d	$-I_a$
$V_{2,30,15,4}$	I_d	$-I_e$	$-I_a$	I_c
$V_{15,8,4,30}$	$-I_a$	I_b	I_c	$-I_e$
$V_{4,29,30,8}$	I_c	$-I_d$	$-I_e$	I_b
$V_{30,16,8,29}$	$-I_e$	I_a	I_b	$-I_d$
$V_{8,27,29,16}$	I_b	$-I_c$	$-I_d$	I_a

Fig. 10 presents the motor speed transient response when the torque reference step is applied. The increase in speed is fast and reaches its set value of 172 r/min at $t = 0.09$ s. When the torque is inverted, the motor changes the rotation direction.

The value of the reference flux is fixed at 1.2 Wb, the representation of Fig. 11 shows that the trajectory of the stator flux is circular, constant equal to its reference value. We also notice that the motor stator flux perfectly follows its reference with good dynamics as shown in Fig. 12.

Fig. 13 and Fig. 14 show the measured and reconstructed phase current values, respectively. The five waveforms may be seen to be similar.

Table 5 Expressions of phase currents

Active Voltage Vector	I_a	I_b	I_c	I_d	I_e
$V_{29,1,16,27}$	I_{dc3}	$I_{dc1}-I_{dc2}-I_{dc3}+I_{dc4}$	$-I_{dc4}$	$-I_{dc1}$	I_{dc2}
$V_{16,23,27,1}$	I_{dc1}	$-I_{dc2}$	$-I_{dc3}$	$-I_{dc1}+I_{dc2}+I_{dc3}-I_{dc4}$	I_{dc4}
$V_{27,2,1,23}$	$I_{dc1}-I_{dc2}-I_{dc3}+I_{dc4}$	$-I_{dc4}$	$-I_{dc1}$	I_{dc2}	I_{dc3}
$V_{1,15,23,2}$	$-I_{dc2}$	$-I_{dc3}$	$-I_{dc1}+I_{dc2}+I_{dc3}-I_{dc4}$	I_{dc4}	I_{dc1}
$V_{23,4,2,15}$	$-I_{dc4}$	$-I_{dc1}$	I_{dc2}	I_{dc3}	$I_{dc1}-I_{dc2}-I_{dc3}+I_{dc4}$
$V_{2,30,15,4}$	$-I_{dc3}$	$-I_{dc1}+I_{dc2}+I_{dc3}-I_{dc4}$	I_{dc4}	I_{dc1}	$-I_{dc2}$
$V_{15,8,4,30}$	$-I_{dc1}$	I_{dc2}	I_{dc3}	$I_{dc1}-I_{dc2}-I_{dc3}+I_{dc4}$	$-I_{dc4}$
$V_{4,29,30,8}$	$-I_{dc1}+I_{dc2}+I_{dc3}-I_{dc4}$	I_{dc4}	I_{dc1}	$-I_{dc2}$	$-I_{dc3}$
$V_{30,16,8,29}$	I_{dc2}	I_{dc3}	$I_{dc1}-I_{dc2}-I_{dc3}+I_{dc4}$	$-I_{dc4}$	$-I_{dc1}$
$V_{8,27,29,16}$	I_{dc4}	I_{dc1}	$-I_{dc2}$	$-I_{dc3}$	$-I_{dc1}+I_{dc2}+I_{dc3}-I_{dc4}$

The simulation results of phase current dynamics during torque inversion are shown in Fig. 15. We can observe that the torque reversal causes a rapid shift in the five currents i_{sa}, i_{sb}, i_{sc}, i_{sd}, and i_{se}.

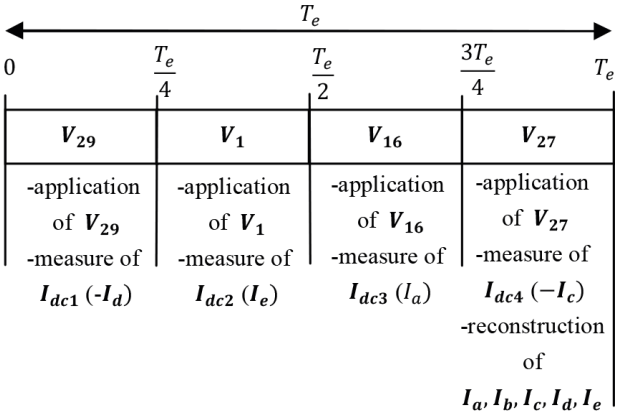

Fig. 8 Four interval of proposal DTC and phase currents reconstruction example with application of $V_{29,1,16,27}$ voltage vector

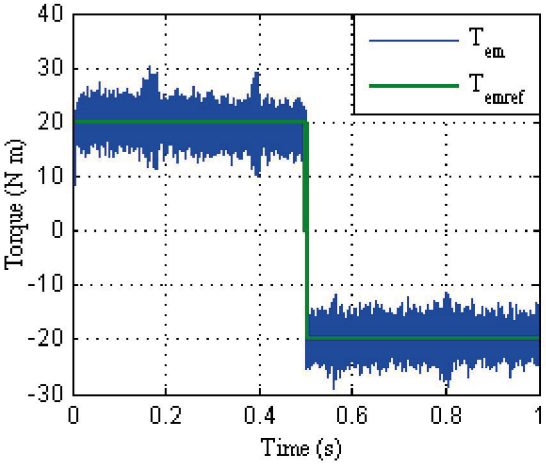

Fig. 9 Motor torque

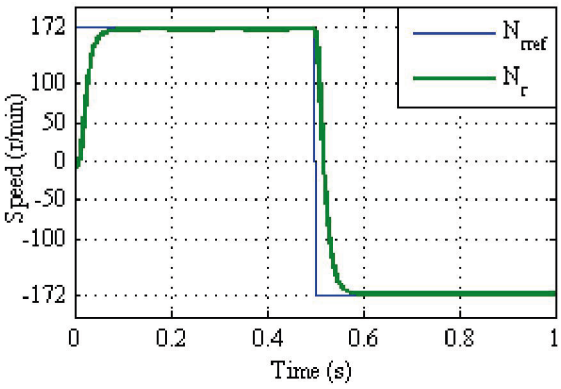

Fig. 10 Speed motor

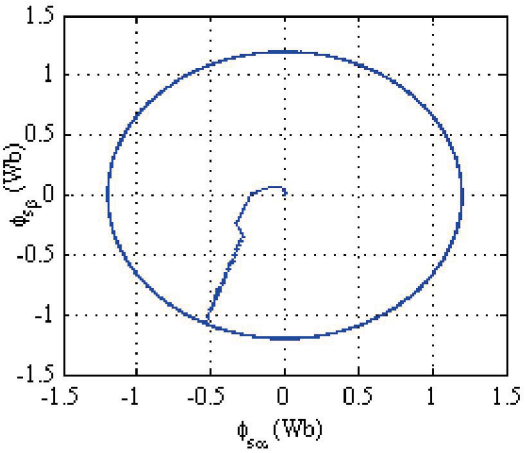

Fig. 11 Stator flux circular trajectory

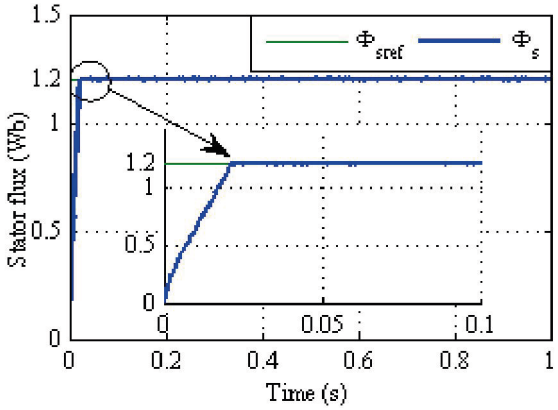

Fig. 12 Stator flux dynamic

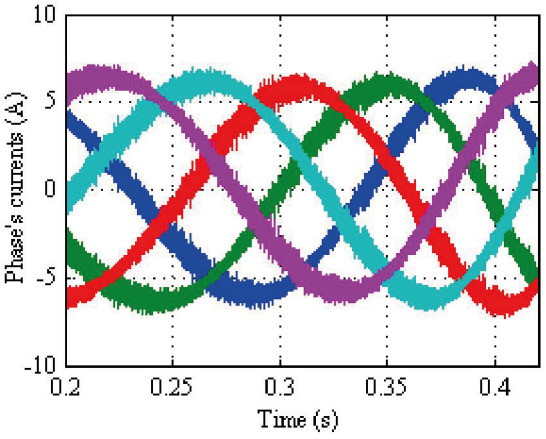

Fig. 13 Measured currents

Fig. 16 shows both measured and reconstructed currents of phase "*a*"; as can be seen, they are identical, and the error value is almost nil.

6 Conclusion

A modified DTC control strategy for driving an FPIM was given in this paper.

The following steps are used to create this modified DTC:

- A careful selection of specific allowable switching vectors generated by a five-phase voltage inverter; by considering just 10 active vectors out of 30, each vector allows for the measurement of one of the motor's five currents during its application.

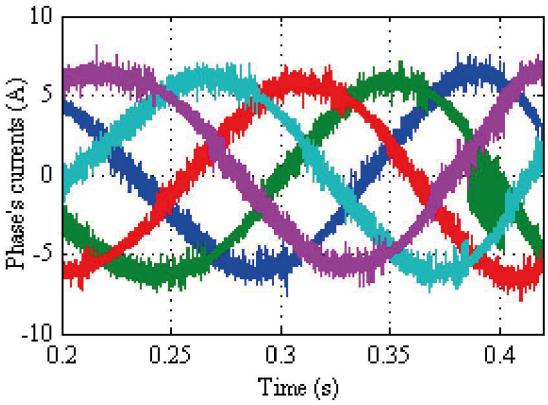

Fig. 14 Constructed currents

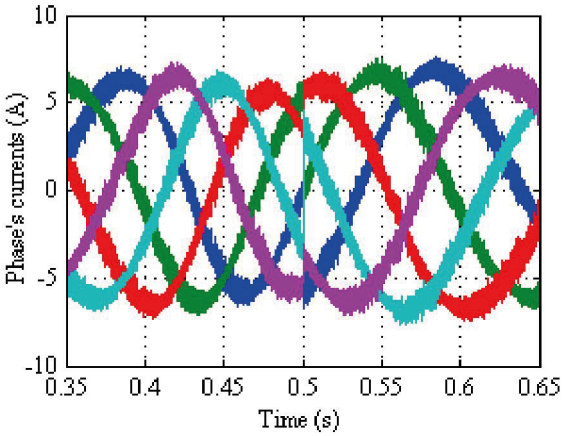

Fig. 15 Phase current dynamic during torque reversal

- The basic scheme of the conventional DTC command is modified using the 18° zone offset strategy, to generate the ten active voltage vectors required for current measurement without modifying the DTC strategy, the four interval discrete vector modulation technique is used.
- A new commutation table has been proposed for the reconstruction of the stator currents necessary for estimating the absolute value of the stator flux and the electromagnetic torque of the motor, by means of a simple DC current sensor placed at the input of the voltage inverter.

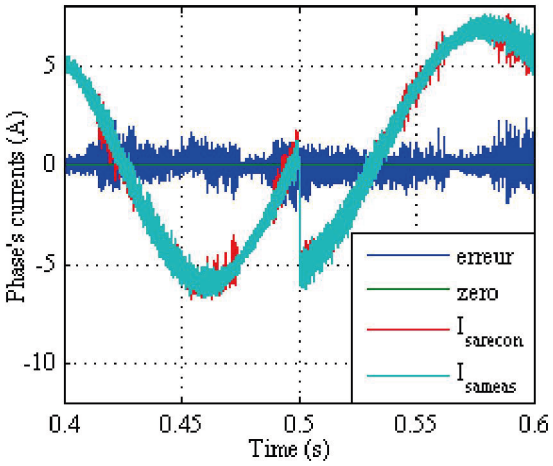

Fig. 16 Zooms of measured and reconstructed currents of phase "*a*"

Finally, we can claim that the dynamic performance was evaluated with the goals of pursuing the reference torque and torque inversion at full load in view. Indeed, simulation results have confirmed the excellent dynamic performances.

References

[1] Levi, E., Bojoi, R., Profumo, F., Toliyat, H. A., Williamson, S. "Multiphase induction motor drives - A technology status review", IET Electric Power Applications, 1(4), pp. 489–516, 2007. https://doi.org/10.1049/iet-epa:20060342

[2] Levi, E. "Multiphase electric machines for variable-speed applications", IEEE Transactions on Industrial Electronics, 55(5), pp. 1893–1909, 2008. https://doi.org/10.1109/TIE.2008.918488

[3] Semail, E., Bouscayrol, A., Hautier, J. P. "Vectorial formalism for analysis and design of polyphase synchronous machines", The European Physical Journal - Applied Physics, 22(3), pp. 207–221, 2003. https://doi.org/10.1051/epjap:2003034

[4] Hasse, K. "Drehzahlregel für schnelle Umkehrantriebe mit stromrichtergespeisten Asynchron-Kurzschlußläufermotoren" (Speed control for fast reversing drives with current-fed rectifier-fed asynchronous squirrel-cage motors), Regelungstechnik und Prozeß-Datenverarbeitung, 20(2), pp. 60–66, 1972. (in German) https://doi.org/10.1524/auto.1972.20.112.60

[5] Blaschke, F. "The principle of fields-orientation as applied to the Transvector closed-loop control system for rotating-field machines", Siemens Review, 34, pp. 217–220, 1972.

[6] Takahashi, I., Noguchi, T. "A new quick-response and high-efficiency control strategy of an induction machine", IEEE Transactions on Industry Applications, IA-22(5), pp. 820–827, 1986. https://doi.org/10.1109/TIA.1986.4504799

[7] Depenbrock, M. "Direct Self-Control of Inverter-Fed Induction Machines", IEEE Transactions on Power Electronics, 3(4), pp. 420–429, 1988. https://doi.org/10.1109/63.17963

[8] Baader, U., Depenbrock, M., Gierse, G. "Direct Self Control (DSC) of Inverter-Fed-Induction Machine: A Basis for Speed Control Without Speed Measurement", IEEE Transactions on Industry Applications, 28(3), pp. 581–588, 1992. https://doi.org/10.1109/28.137442

[9] Foo, G., Rahman, M. F. "Direct torque and flux control of an IPM synchronous motor drive using a backstepping approach", IET Electric Power Applications, 3(5), pp. 413–421, 2009. https://doi.org/10.1049/iet-epa.2008.0182

[10] Haque, M. E., Rahman, M. F. "Incorporating control trajectories with the direct torque control scheme of interior permanent magnet synchronous motor drive", IET Electric Power Applications, 3(2), pp. 93–101, 2009. https://doi.org/10.1049/iet-epa:20070518

[11] Metidji, B., Taib, N., Baghli, L., Rekioua, T., Bacha, S. "Low-cost direct torque control algorithm for induction motor without AC phase current sensors", IEEE Transactions on Power Electronics, 27(9), pp. 4132–4139, 2012. https://doi.org/10.1109/TPEL.2012.2190101

[12] Moati, Y., Kouzi, K. "Investigating the Performances of Direct Torque and Flux Control for Dual Stator Induction Motor with Direct and Indirect Matrix Converter", Periodica Polytechnica Electrical Engineering and Computer Science, 64(1), pp. 97–105, 2020. https://doi.org/10.3311/PPee.14977

[13] Azib, A., Ziane, D., Rekioua, T. "Ensure continuity of operation of an electric vehicle under fault condition in converter", International Journal of Hydrogen Energy, 41(21), pp. 9066–9074, 2016. https://doi.org/10.1016/j.ijhydene.2016.03.162

[14] Zheng, L., Fletcher, J. E., Williams, B. W., He, X. "A Novel Direct Torque Control Scheme for a Sensorless Five-Phase Induction Motor Drive", IEEE Transactions on Industrial Electronics, 58(2), pp. 503–513, 2011. https://doi.org/10.1109/TIE.2010.2047830

[15] Muduli, U. R., Chikondra, B., Behera, R. K. "Space Vector PWM Based DTC Scheme With Reduced Common Mode Voltage for Five-Phase Induction Motor Drive", IEEE Transactions on Power Electronics, 37(1), pp. 114–124, 2022. https://doi.org/10.1109/TPEL.2021.3092259

Appendix

The parameters of the FPIM used in this study are as follows:

- Power: P_n = 3.5 Kw,
- Base speed: N_r = 1461 rpm,
- Stator winding resistance: R_s = 2.47 Ω,
- Rotor winding resistance: R_r = 1.8 Ω,
- Stator Leakage inductance: L_{ls} = 4 mH,
- Rotor Leakage inductance: L_{lr} = 4 mH,
- Mutual inductance: L_m = 0.226 H,
- Number of pole pairs: p = 2,
- Moment of inertia: J = 0.09 Kg m^2.